Midinfrared and Quantum-Chemical Study of the Structure, Conformation, and Isomerization of the Unstable CH_3CH_2OCN Molecule

Tibor Pasinszki,*,† Balázs Havasi,† and Attila Kovács‡

Department of Inorganic Chemistry, Budapest University of Technology and Economics, H-1521 Budapest, Gellért tér 4, Hungary, and Research Group for Technical Analytical Chemistry of the Hungarian Academy of Sciences at the Institute of General and Analytical Chemistry, Budapest University of Technology and Economics, H-1521 Budapest, Gellért tér 4, Hungary

Received: May 14, 2002; In Final Form: December 2, 2002

Gaseous ethyl cyanate, CH_3CH_2OCN, has been generated from the gas/solid reaction of *O*-ethyl thiocarbamate with mercury oxide and characterized in the gas phase by infrared spectroscopy for the first time. Experimental data indicate the presence of two conformers in the gas phase, the gauche (synclinal) and the trans (antiperiplanar) form. The molecular geometries and energetics of the possible conformers are obtained from DFT calculations at the B3LYP level and from ab initio calculations at the MP2, MP3, MP4, QCISD, and CCSD(T) levels of theory. The assignment of the gas-phase infrared spectrum is assisted by normal coordinate calculations based on the scaled computed force field of the two conformers. The kinetic instability of CH_3CH_2OCN toward isomerization is studied at the B3LYP level, in a vacuum and in solutions. Solvent effects are modeled using the polarized continuum model (PCM). Calculations show that the isomerization is not a unimolecular process at ambient temperatures, and bimolecular processes are responsible for the instability. In polar solvents, the OCN^- anion plays a key role in the isomerization, being an effective catalyst for the cyanate-isocyanate rearrangement.

Introduction

Covalent cyanates (R−O−C≡N) are in general unstable compounds and isomerize into their thermodynamically more stable isocyanate derivatives. The cyanate structure is stable only in special cases, e.g., if the substituent, *R*, is an aryl group,[1,2] or the substituent is bulky, preventing the isomerization sterically.[3,4] Ethyl cyanate, CH_3CH_2OCN, is no exception. It isomerizes readily at room or higher temperatures,[5] and the process is believed to be autocatalyzed by the isomer.[1] Because of instability, its application in chemical reactions requires an in situ generation or prior to use, and it must be stored at low temperatures.[6]

Because ethyl cyanate is unstable, little is known experimentally about its structure and spectroscopy. The IR[7,8] and NMR[8] spectra were, however, recorded in cold CCl_4 solution, and the only gas-phase investigations are the early mass[9] and recent microwave[10] spectroscopic study. In the microwave work, by comparing the experimental rotational constants to those of model geometries, the observed spectrum was assigned to the trans (antiperiplanar) conformer. The search for another conformer among the weak spectral lines was unsuccessful; therefore, the trans conformer was concluded to be the most stable. No geometrical parameters could be derived from the experimental data, because of insufficient number of isotope substitutions.

Because of the lack of detailed experimental work, quantum chemical calculations become important in providing information on the conformers of CH_3CH_2OCN. The four possible conformers for this molecule can be derived by a rotation around the $C(H_2)-O$ single bond: cis (synperiplanar), gauche (synclinal), skew (anticlinal), and trans (antiperiplanar) forms with CCOC dihedral angles of 0°, ∼60°, ∼120°, and 180°, respectively. The structures of the cis, gauche, and trans conformer were calculated recently at the HF and MP2 levels, neglecting, however, the skew conformer.[11] These calculations predicted the gauche and trans forms to be minima on the potential energy surface, whereas the cis form turned out to be a transition state. The calculated energy difference between the gauche and trans conformers was small, favoring the gauche at the MP2 and the trans at the HF and MP4//MP2 (single-point MP4 calculation at the MP2 geometry) levels.[11]

Alkyl cyanates are known to isomerize at ambient temperatures,[1,12] although the mechanism of this process is not yet understood. The only work addressing this question so far is that of Martin et al.,[1] where the kinetics of the isomerization of ethyl cyanate was investigated in various solvents and temperatures. It has been observed that the speed of isomerization is influenced by solvents and depends on the concentration. In nonpolar aprotic solvents (diethyl ether, CH_3Cl, CCl_4, benzene, and toluene), CH_3CH_2OCN is fairly stable and can be stored in a refrigerator for weeks. The half-life of CH_3CH_2OCN in toluene is 654 and 232 min at 79.5 and 91 °C, respectively. During the rearrangement, the formation of both ethyl isocyanate and triethylisocyanurate (ethyl isocyanate trimer) is observed. In polar solvents (nitrobenzene, acetonitrile), the isomerization is ca. 20-times faster than in toluene and the formation of ethylisocyanurate is not observed at 73.5 °C over a time of 140 min. In dimethylformamide (DMF), CH_3CH_2OCN isomerizes rapidly at room temperature (half-lives at 0 and 9 °C are 441 and 75 min, respectively), and the speed of isomerization is ca.

* To whom correspondence should be addressed. E-mail: pasinszki@mail.bme.hu.

† Department of Inorganic Chemistry, Budapest University of Technology and Economics.

‡ Research Group for Technical Analytical Chemistry of the Hungarian Academy of Sciences at the Institute of General and Analytical Chemistry, Budapest University of Technology and Economics.

10.1021/jp0211990 CCC: $25.00
Published on Web 02/25/2003

SCHEME 1

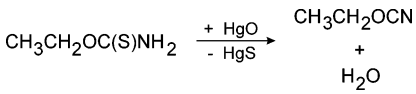

3−4 order of magnitude higher than in nitrobenzene or acetonitrile. The isomerization in dimethyl sulfoxide (DMSO) and DMF is fast at room temperature, and the major isolated product from the reaction mixture is triethylisocyanurate. One of the key experiments on this subject was the investigation of the isomerization of an equimolar mixture of $C_2H_5OC^{15}N$ and *n*-C_4H_9OCN in nitrobenzene, which indicated the equimolar formation of $C_2H_5{}^{15}NCO$ and *n*-$C_4H_9{}^{15}NCO$.[1] On the basis of this and experiments discussed above, it have been suggested that the isomerization proceeds via a solvent separated ion pair $[C_2H_5{}^+|OCN^-]$. It has also been noted that the formation of free solvated $C_2H_5{}^+$ and OCN^- ions is not expected because of the weak ionizing power of nitrobenzene.[1]

The aim of the present study is to generate and characterize CH_3CH_2OCN in the gas phase, to derive information about the structure and energetics of its conformers, and to obtain information about its stability and isomerization. To this end, CH_3CH_2OCN is studied in the gas phase by mid-infrared (IR) spectroscopy and the experimental work is complemented by extensive quantum-chemical calculations.

Experimental Section

A mixture of gaseous ethyl cyanate and water was generated by passing *O*-ethyl thiocarbamate[13] over solid yellow mercury-(II) oxide (FERAK Laborat GMBH) packed into a small Pyrex tube (Scheme 1).[10,12] The CH_3CH_2OCN/H_2O mixture from the reaction zone was led directly into the IR spectrometer or condensed in a U-trap inserted between the reaction tube and the spectrometer.

Mid-IR spectra (4000−500 cm^{-1}, 1 cm^{-1} resolution) were collected on a Perkin-Elmer System 2000 Fourier transform spectrometer equipped with a mercury cadmium telluride (MCT) detector. Measurements were performed at room temperature using a 240 cm multipass gas cell with KCl windows (PikeTech). The effluent from the reaction tube or the sample from the U-trap was continuously pumped through the cell using a rotary pump while maintaining the pressure between 550 and 600 mTorr. The IR spectra of gaseous *O*-ethyl thiocarbamate and CH_3CH_2NCO (Aldrich) were recorded on a similar manner.

Computational Methods

Theoretical calculations for the structure of CH_3CH_2OCN were carried out first using the density functional theory, DFT, in the form of B3LYP (Becke's three-parameter exchange functional in combination with Lee, Yang, and Parr correlation functional). The conformers of CH_3CH_2OCN and the interconnecting transition states (TS) with respect to the C(ethyl)−O single bond were investigated at the B3LYP/6-311+G(2d,2p) level. Equilibrium molecular geometries were fully optimized, and the existence of true minima was confirmed by harmonic frequency analysis (zero imaginary frequency). TSs were characterized by one imaginary frequency. The potential energy curve of the torsional motion was obtained by proceeding along the given reaction coordinate and simultaneously relaxing all other bond lengths and angles. Geometries of the minimum energy structures (gauche and trans forms) and transition states (cis and skew forms) were also optimized at the MP2(full)/6-311+G(2d,2p) level, and structures of the gauche and trans conformers were additionally calculated at the HF/6-311+G-(2d,2p), MP3(full)/6-311+G(2d,2p), QCISD(full)/6-311+G-(d,p), and MP4(full)/6-31G(d,p) levels. These latter geometry optimizations were extended by harmonic frequency calculations at the HF, MP2, and QCISD levels. To have a better estimate of the relative energies of the conformers, single-point calculations were performed on the optimized B3LYP, MP2, MP4, and QCISD structures at the MP4(full)/6-311+G(2d,2p) and CCSD(T)(full)/6-311+G(2d,2p) levels, denoted as MP4//MP4, CCSD(T)//B3LYP, CCSD(T)//MP2, CCSD(T)//MP4, and CCSD-(T)//QCISD. For testing the reliability of theoretical levels used, calculations were done for the geometry of CH_3OCN, at the same levels used for CH_3CH_2OCN, and results were compared to the available experimental microwave structure.

Unimolecular isomerization and intermolecular reactions of CH_3CH_2OCN were modeled in a "vacuum" and in the presence of a solvent at the B3LYP/6-311+G(2d,2p) level. Five solvents were selected from the available solvent list in Gaussian 98: heptane (dielectric constant: $\epsilon = 1.92$), dichloroethane ($\epsilon = 10.36$), acetone ($\epsilon = 20.7$), nitromethane ($\epsilon = 38.2$), and DMSO ($\epsilon = 46.7$). Solvent effects were calculated using the popular PCM as incorporated in Gaussian 98. All calculations were carried out with the Gaussian 98 quantum chemistry package[14] implemented on a Silicon Graphics Inc. Origin 200 workstation.

Computational Details of the SQM Analysis. The scaled quantum mechanical (SQM) analysis[15] of ethyl cyanate was based on the computed harmonic B3LYP/6-311+G(2d,2p) force field in a nonredundant internal coordinate representation.[16] The Cartesian force field was transformed to internal coordinates using the program TRA3.[17] For the scaling scheme, Pulay's standard (selective) scaling method[18] was used. The solution of the secular equation and optimization of the scale factors were done with the program SCALE3.[19,20] For characterization of the fundamentals, their total energy distribution (TED)[21,22] was used which provides a measure of each internal coordinate's contribution to the normal coordinate in terms of energy.

Results and Discussion

Theoretical Calculations. The electronic and geometric structures of pseudohalides are known to be sensitive to electron correlation effects, often presenting a serious challenge for quantum chemical methods. The effect of electron correlation on the calculated structure depends on the kind of molecule investigated, hence the methods used for a systematic study of a certain type of pseudohalide must be tested prior to use. The simplest method is to compare calculated quantities to experimental data, keeping in mind that the calculated equilibrium structure (r_e) is usually compared to a vibrationally averaged experimental structure (r_0, r_s, r_a, r_g, etc.). Experimental information about the geometry of covalent cyanates is very scarce; CH_3OCN[23] and F_5SOCN[24] are the only derivatives with known gas-phase structures. We note that, although an r_a structure was published for F_5SeOCN,[25] it is still ambiguous whether the cyanate, and not the isocyanate, is synthesized and studied. The performance of various computational levels for selected covalent cyanates is compared in Table 1, which shows, that the calculated bond lengths are sensitive to the theoretical level used, especially for the C≡N triple bond. The HF method underestimates the C≡N bond length, MP2 and MP4 overestimate it, and a clear oscillation can be seen within the MP expansion series. The QCISD method also seems to overestimate the C≡N bond length, although to a lesser extent than MP2 or MP4. The B3LYP geometry is in the best agreement with experimental MW data. When the calculated structure of CH_3CH_2OCN is compared to that of CH_3OCN, the same trends are

TABLE 1: Comparison of the Structural Characteristics of Selected Covalent Cyanates

molecule/method	C−O (Å)	O−C (Å)	C≡N (Å)	OCN (deg)	COC (deg)
CH_3OCN (MW r_s)[a]	1.455	1.302	1.146	178.4	113.8
F_5SOCN (ED, r_a)[b]		1.271	1.162	175.3	
CH_3OCN (r_e)[c]					
B3LYP	1.459	1.288	1.156	178.0	115.3
HF	1.436	1.272	1.129	179.4	115.7
MP2	1.454	1.294	1.173	178.2	113.3
MP3	1.445	1.291	1.151	178.7	113.7
MP4	1.457	1.307	1.185	178.3	113.4
QCISD	1.449	1.295	1.164	178.7	113.5
CH_3CH_2OCN (r_e)[c,d]					
B3LYP	1.476	1.287	1.156	178.2	115.6
HF	1.448	1.272	1.130	179.4	115.9
MP2	1.466	1.293	1.174	178.3	113.4
MP3	1.457	1.291	1.151	178.7	113.8
MP4	1.469	1.306	1.186	178.6	113.6
QCISD	1.460	1.294	1.164	178.7	113.6

[a] Ref 23a (from microwave spectroscopy, MW). [b] Ref 24 (from electron diffraction, ED). [c] This work. [d] Trans conformer.

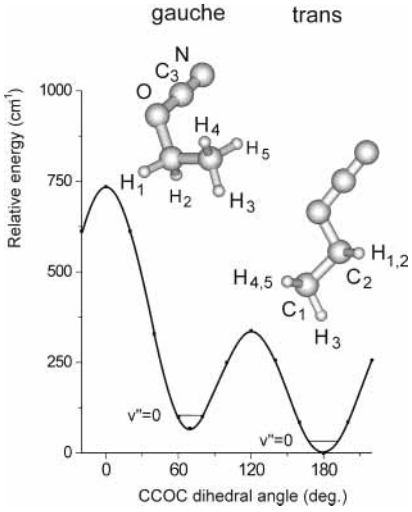

Figure 1. Structures, numbering of the atoms, the deformation potential, and relative energies of the conformers of CH_3CH_2OCN. Ground vibrational levels are estimated from harmonic frequency calculations.

observed. We note a similar performance of the computational methods in the case of nitrile oxides, R−C≡N → O, one of the isomers of cyanates.[26−28] We have observed and pointed out recently[27−29] that B3LYP is capable of describing the equilibrium structure of the nitrile oxides, and DFT methods provide an efficient alternative for calculating the structure if high level ab initio methods are computationally not feasible. On the basis of the analogy between CH_3OCN and CH_3CH_2OCN, we can assume the same behavior of the tested computational methods for describing the molecular geometry and electronic structure of CH_3CH_2OCN.

The calculated structure of CH_3CH_2OCN is shown in Figure 1 with calculated bond lengths and angles listed in Table 2. According to our calculations, CH_3CH_2OCN has two stable conformers, the gauche and the trans forms, whereas the cis and skew are transition states on the potential energy surface. Table 3 lists the relative energies of conformers. The trans form is thermodynamically favored at the HF (not shown in Table 3), MP3, B3LYP, QCISD, and CCSD(T) levels, and only MP4 and MP2 calculations are in disagreement. However, using a larger basis set in the MP4 calculation and taking into account ZPE and thermal corrections (ΔG), the trans is also favored at

TABLE 2: Calculated Equilibrium Structures, Total Energies, Dipole Moments, and Rotational Constants of Gauche and *trans*-CH_3CH_2OCN[a]

	gauche r_e	trans r_e	trans expt. (r_0)[b]
C_1-C_2	1.511 (1.516)	1.507 (1.513)	
C_2-O	1.477 (1.461)	1.476 (1.460)	
$O-C_3$	1.286 (1.294)	1.287 (1.294)	
C_3-N	1.156 (1.165)	1.156 (1.164)	
C_2-H_1	1.086 (1.091)	1.089 (1.094)	
C_2-H_2	1.089 (1.095)	1.089 (1.094)	
C_1-H_3	1.091 (1.095)	1.090 (1.095)	
C_1-H_4	1.089 (1.094)	1.089 (1.094)	
C_1-H_5	1.089 (1.094)	1.089 (1.094)	
C_1C_2O	111.7 (111.4)	107.3 (107.0)	
C_2OC_3	115.6 (113.9)	115.6 (113.6)	
OC_3N	178.2 (178.7)	178.2 (178.7)	
H_1C_2O	102.8 (103.3)	107.4 (108.0)	
H_2C_2O	107.4 (108.0)	107.4 (108.0)	
$H_3C_1C_2$	109.1 (109.2)	109.1 (109.2)	
$H_4C_1C_2$	111.0 (110.5)	111.0 (110.6)	
$H_5C_1C_2$	111.2 (111.1)	111.0 (110.6)	
C_2OC_3N	180.0 (180.0)	180.0	
$C_1C_2OC_3$	69.5 (66.8)	180.0	
total energy:	−247.345617 (−246.781627)	−247.345934 (−246.781654)	
μ[c]	4.92 (4.60)	5.13 (5.17)	4.72
A[d]	12.4348 (11.9157)	31.0545 (30.5102)	30.055
B	3.3949 (3.5213)	2.5172 (2.5381)	2.54353
C	2.9007 (2.9593)	2.3986 (2.4150)	2.41967

[a] Calculated at the B3LYP/6-311+G(2d,2p) and QCISD(full)/6-311+G(d,p) (in parentheses) levels. Bond angles are in degrees; bond lengths are in Å; total energies are in a.u.; see Figure 1. [b] From microwave spectrum (ref 10). [c] Dipole moments in Debye. [d] Rotational constants in GHz. Isotopes: ^{12}C, ^{1}H, ^{14}N, and ^{16}O.

MP4. There is an oscillation in the HF = MP1 → MP2 → MP3 → MP4 series regarding the gauche−trans relative energy, similar to the oscillation in bond lengths. On the basis of the calculated results summarized in Table 3, especially on that of the highest CCSD(T)//B3LYP level, we conclude that the major conformer at room temperature is the trans one. However, the energy difference between the two minima is small, and because the interconnecting skew transition state is also rather low in energy, there must be a thermal equilibrium between the gauche and trans conformers in the gas phase. Calculations at various levels in Table 3 predict a gauche/trans ratio of 0.54−1.09/1, so both conformers may be observable in a sample at room temperature. The major component trans form has been observed in the previous microwave work,[10] supported by the present calculated rotational constants in Table 2. We note that, because B3LYP provides good equilibrium geometries for pseudohalides and CCSD(T) provides the best estimate of the total energy, we believe that the best estimate of the conformer ratio is given by the CCSD(T)//B3LYP method (0.76/1). Our IR spectroscopic investigation (see below) suggests the presence of both conformers in a room-temperature sample. Figure 1 shows the relative energies of the various conformers of CH_3CH_2OCN and the C−O torsional potential calculated at the B3LYP level. In this figure, the $\nu'' = 0$ level is marked, on the basis of the calculated (torsional) zero-point vibrational energy. The calculated harmonic torsional frequency is 61 and 77 cm^{-1} for the trans and gauche conformer, respectively, so it is expected that a hindered torsional motion exists around the gauche and trans minima in the ground and lowest lying excited states (i.e., $\nu'' = 1-3$) of this vibration, which may become free only at higher levels of excitation.

Identification and Infrared Spectrum of CH_3CH_2OCN. An important aspect of this work is to show that pure ethyl cyanate has been generated for IR investigation and that it is

TABLE 3: Calculated Relative Energies (ΔE)[a] and Gibbs Free Energies (ΔG)[b] (kJ/mol) of CH_3CH_2OCN Conformers

	ΔG (ΔE)				
level of theory	cis TS	gauche	skew TS	trans	gauche/trans ratio[c]
B3LYP	11.70 (*8.67*)	1.52 (*1.27*)	7.17 (*3.87*)	0.00 (*0.00*)	0.54/1
QCISD	*g*	1.41 (*0.61*)	*g*	0.00 (*0.00*)	0.57/1
MP2	10.07 (*7.44*)	0.07 (*0.00*)	7.95 (*5.13*)	0.00 (*0.22*)	0.97/1
MP3[d]	*g*	0.86 (*0.56*)	*g*	0.00 (*0.00*)	0.71/1
MP4[d]	*g*	0.00 (*0.00*)	*g*	0.20 (*0.50*)	1/0.92
MP4//MP4[d]	*g*	0.20 (*0.00*)	*g*	0.00 (*0.09*)	0.92/1
CCSD(T)//MP4[d]	*g*	0.47 (*0.18*)	*g*	0.00 (*0.00*)	0.83/1
CCSD(T)//MP2[d]	10.85 (*7.99*)	0.50 (*0.21*)	7.82 (*4.78*)	0.00 (*0.00*)	0.82/1
CCSD(T)//B3LYP[e]	11.19 (*8.16*)	0.69 (*0.44*)	8.04 (*4.74*)	0.00 (*0.00*)	0.76/1
CCSD(T)//QCISD[f]	*g*	1.18 (*0.38*)	*g*	0.00 (*0.00*)	0.62/1

[a] Zero-point vibrational energy (ZPE) is added to the total energy. [b] Calculated at temperature of 298.15 K and pressure of 1.0 Atm. [c] Calculated using ΔG values and the Boltzman equation. [d] ZPE and thermal corrections are calculated at the MP2/6-311+G(2d,2p) level. [e] ZPE and thermal corrections are calculated at the B3LYP/6-311+G(2d,2p) level. [f] ZPE and thermal corrections are calculated at the QCISD/6-311+G** level. [g] Not calculated.

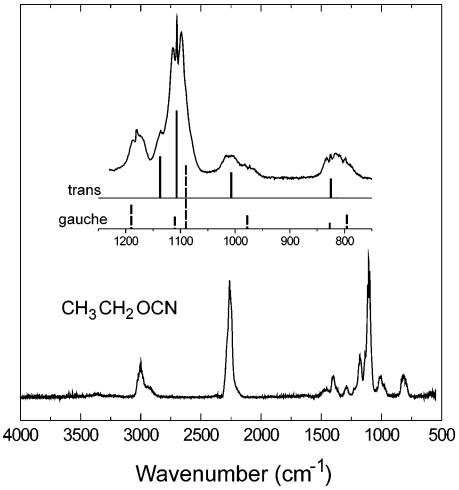

Figure 2. Infrared spectrum of gaseous CH_3CH_2OCN. Inset shows the expanded 1250−750 cm^{-1} region together with calculated band positions and relative IR intensities (scaled frequencies are from Table 4).

not contaminated with the isocyanate isomer, *O*-ethyl thiocarbamate precursor, or any other side product. To this end, an authentic sample of the stable CH_3CH_2NCO isomer and the precursor *O*-ethyl thiocarbamate were also investigated by IR spectroscopy under the same conditions. We note that the reaction could be monitored visually following the formation of black HgS from yellow HgO and the reaction was stopped before the black zone of HgS reached the end of the reaction tube. Supporting the 100% conversion in the above reaction, no evidence was found for residual starting material in the IR spectrum. In a separate experiment, the effluent from the reaction tube was condensed at −78 °C in a U-trap, and this was then gradually warmed allowing the detection of reaction products in the order of their relative volatility. The most volatile side product, the isocyanate isomer, was observed only in trace amounts and was pumped off before recording the spectrum of CH_3CH_2OCN. CH_3CH_2OCN had sufficient vapor pressure at 0 °C for IR investigation, and no indication of isomerization were observed at this temperature during the measurement.

The IR spectrum of gaseous CH_3CH_2OCN is shown in Figure 2 with observed and calculated frequencies listed in Table 4. For a better assistance in assignment of the spectrum, the computed harmonic frequencies are corrected using the popular scaled quantum mechanical (SQM) method of Pulay et al., where the computed harmonic force field is improved by a small number of properly chosen transferable scale factors.[15] Such general scale factors have been developed for the B3LYP/6-31G* level,[30,31] but we are not aware of any transferable scale factors for our B3LYP/6-311+G(2d,2p) level. Because the scale factors are known to be well transferable between very closely related derivatives, we have developed the necessary scale factors on the basis of the known gas-phase IR data of the analogous CH_3OCN.[12] The optimized scale factors for CH_3 stretch, OC stretch, C≡N stretch, C_{et}−O stretch, HCH bend, and CCH bend are given in the footnote to Table 4. In the lack of experimental information, no scale factors could be developed for the low-frequency bending and torsional internal coordinates and for the C−C stretch; thus, we kept these scale factors at the preliminary value of 1.000. We note that the optimized scale factors are close to unity, which reflects the high quality of the unscaled B3LYP/6-311+G(2d,2p) force field.

The gas-phase IR spectrum of CH_3CH_2OCN (Figure 2) concurs in general with that previously obtained in CCl_4 solution[8] and shows two strong features at 2255 and 1106 cm^{-1} corresponding to the C≡N and O−C(N) stretches, which are the most characteristic fingerprints of the cyanate group (note the alternative description of OCN asymmetric and symmetric stretches, respectively). These bands show *B*/*A*- and *A*/*B*-type band structure with ca. 14 and 15 cm^{-1} PR separation, respectively, in agreement with the calculated values.[32] The spectrum shows other peaks with medium to small intensity corresponding to CH stretches (around 3000 cm^{-1}), CH_3 and CH_2 deformations (1500−1100 cm^{-1} region), and C−C and C−O stretches (1000−820 cm^{-1} region). Assignments of IR bands are listed in Table 4.

A crucial question is whether both stable conformers, the gauche and the trans, can be identified in the experimental IR spectrum. It is not straightforward to decide in this question because most of the fundamentals of the two conformers lie close to each other with similar intensities. The most straightforward proof of the coexistence of the two conformers is found in the 1200−800 cm^{-1} spectral region (see inset to Figure 2). The scaled calculated frequency of the O−C(N) stretch of the trans conformer matches the position of the strong Q branch in the spectrum at 1106 cm^{-1}, so we assign this band to the trans conformer. The partially overlapped bands at 1136, 1008, and 825 cm^{-1} are also assigned to the trans conformer, on the basis of calculated frequencies, IR intensities, and conformer ratio. The band at 1180 cm^{-1} with medium intensity and the weak bands at 974 and 798 cm^{-1} clearly show the presence of the gauche conformer. We note that there are other indications of the presence of two conformers. The weak bands at 1377 and 1290 cm^{-1} can only be explained with the presence of the trans and gauche conformers, respectively. The strong band at 2255

TABLE 4: Experimental and Calculated Vibrational Frequencies (cm^{-1}) of CH_3CH_2OCN

	trans[b]				gauche[b]			
expt frequency[a]	frequency[c]	intens[d]		assignment and TED[e]	frequency[c]	intens[d]		assignment and TED[e]
3021 Q m					3027 (3150)	14.2	ν_1	78% CH_2 asst, 13% CH_3 asst
3007 Q m	3011 (3134)	24.3	ν_{16}	65% CH_3 asst, 35% CH_2 asst				
2997 Q m	2995 (3117)	14.2	ν_1	98% CH_3 asst	2996 (3119)	8.8	ν_2	87% CH_3 asst
2989 Q w	2986 (3108)	1.0	ν_{17}	65% CH_2 asst, 35% CH_3 asst	2987 (3110)	11.9	ν_3	95% CH_3 asst
(2963)	2945 (3065)	13.5	ν_2	98% CH_2 sst	2957 (3078)	16.0	ν_4	85% CH_2 sst, 11% CH_2 asst
2934 w	2933 (3052)	6.8	ν_3	100% CH_3 sst	2928 (3047)	5.3	ν_5	99% CH_3 sst
2262 R 2255 Q vs 2248 P	2259 (2337)	225.9	ν_4	83% C≡N st, 17% OC st	2257 (2334)	201.7	ν_6	83% C≡N st, 17% OC st
	1506 (1520)	6.2	ν_5	95% CH_2 sci	1501 (1516)	5.6	ν_7	92% CH_2 sci
1480 w	1479 (1506)	2.5	ν_6	78% CH_3 asd	1477 (1503)	0.9	ν_8	77% CH_3 asd
1454 w	1460 (1490)	7.7	ν_{18}	89% CH_3 asd, 11% CH_3 r	1462 (1492)	7.7	ν_9	88% CH_3 asd, 11% CH_3 r
1401 m	1418 (1430)	24.1	ν_7	72% CH_3 sd, 14% CH_2 w	1414 (1426)	15.8	ν_{10}	81% CH_3 sd
1377 w	1391 (1403)	12.2	ν_8	77% CH_2 w, 20% CH_3 sd	1387 (1400)	2.9	ν_{11}	84% CH_2 w, 12% CH_3 sd
1290 w	1289 (1300)	0.7	ν_{19}	79% CH_2 tw, 17% CH_3 r	1306 (1317)	13.3	ν_{12}	84% CH_2 tw, 11% CH_3 r
1180 Q m	1161 (1171)	4.2	ν_{20}	54% CH_2 r, 30% CH_3 r, 11% CH_2 tw	1190 (1203)	43.9	ν_{13}	47% CH_2 r, 33% CH_3 r
1136 sh	1137 (1121)	63.6	ν_9	27% CH_3 r, 25% OC st, 21% CC st				
1113 R 1106 Q vs 1098 P	1107 (1158)	133.1	ν_{10}	42% OC st, 20% C−O st, 19% CH_3 r	1110 (1105)	22.5	ν_{14}	41% CH_3 r, 14% CC st, 13% OC st
					1090 (1124)	115.7	ν_{15}	39% OC st, 24% CC st, 14% C−O st
1008 m	1007 (1008)	39.3	ν_{11}	56% CC st, 15% CH_3 r, 15% CO st				
974 w					978 (983)	24.6	ν_{16}	47% CC st, 22% CH_3 r, 12% OC st
825 Q m	825 (821)	29.6	ν_{12}	51% C−O st, 22% CH_3 r	827 (828)	10.9	ν_{17}	29% C−O st, 29% CH_3 r, 16% CH_2 r
	814 (821)	1.3	ν_{21}	44% CH_2 r, 42% CH_3 r				
798 Q m					796 (796)	25.7	ν_{18}	33% C−O st, 26% CH_2 r, 23% CH_3 r
	597 (596)	5.2	ν_{13}	52% OCN b, 30% CCO b, 12% C−O st	622 (622)	4.0	ν_{19}	46% OCN b, 35% CCO b
	528 (528)	8.1	ν_{22}	100% OCN b	532 (532)	9.9	ν_{20}	97% OCN b
	378 (379)	6.1	ν_{14}	69% COC b, 10% OCN b	395 (396)	0.8	ν_{21}	74% COC b, 13% OCN b
	242 (243)	0.1	ν_{23}	97% CC t	270 (271)	1.8	ν_{22}	73% CC t, 12% CCO b, 11% OCN b
	177 (177)	4.9	ν_{15}	55% CCO b, 32% OCN b, 12% COC b	188 (188)	5.0	ν_{23}	45% CCO b, 25% OCN b, 23% CC t
	61 (61)	1.8	ν_{24}	100% C−O t	77 (77)	0.9	ν_{24}	100% C−O t

[a] For the relative intensities see also Figure 3. [b] Calculated at the B3LYP/6-311+G(2d,2p) level. [c] Scaled frequencies (see text). Scale factors used in the SQM analysis: CH_3 st: 0.9231, OC st: 0.9285, CN st: 0.9371, C−O st: 1.0378, CC st: 1.0000, HCH b: 0.9577, CCH b: 0.9846, COC b: 1.0000, OCN lin. b: 1.0000, CH_3 t: 1.0000. Unscaled harmonic frequencies are in parentheses. [d] In km/mol. [e] Characterization of the fundamentals: total energy distribution (TED). Only contributions above 10% are given. The abbreviations sst, asst, st, sd, asd, b, sci, r, tw, w, t mean symmetric stretching, asymmetric stretching, stretching, symmetric deformation, asymmetric deformation, bending, scissoring, rocking, twisting, wagging and torsion, respectively. Scaled force constants were used.

TABLE 5: Calculated Barriers (TS2) of the Bimolecular Reaction of CH_3CH_2OCN and Energetics (D2) for the Bimolecular Formation of OCN^- Ion[a]

solvent	TS2a[ΔG (ΔE)], kJ/mol	TS2b[ΔG (ΔE)], kJ/mol	TS2c[ΔG (ΔE)], kJ/mol	D2[ΔG (ΔE)][b], kJ/mol
vacuum	172.9 (128.0)	169.7 (124.4)	*c*	418.1 (425.9)
heptane	173.6 (131.5)	161.1 (128.7)	*c*	223.1 (230.5)
dichloroethane	155.6 (112.9)	145.9 (110.4)	155.2 (109.9)	62.0 (56.6)
acetone	151.8 (110.5)	140.3 (109.3)	140.2 (107.7)	39.4 (36.9)
nitromethane	153.2 (112.4)	139.1 (108.8)	145.6 (107.8)	34.0 (29.8)
DMSO	152.3 (112.8)	141.3 (109.7)	148.4 (110.1)	32.3 (27.8)

[a] Calculated at the B3LYP/6-311+G(2d,2p) level. Energies (including ZPE) and Gibbs free energies (298 K, 1 atm) are relative to that of the sum of two CH_3CH_2OCN molecules; TS2a: barrier to two molecules of CH_3CH_2NCO, TS2b: barrier to the dimer, DP, TS2c: barrier to the formation of OCN^- ion. [b] Energetics is determined for the $CH_3CH_2OCN + CH_3CH_2OCN \rightarrow CH_3CH_2OCNCH_2CH_3^+ + OCN^-$ reaction. [c] Not calculated.

cm^{-1} has an unusual contour showing a shoulder at 2278 cm^{-1}. Although there are several strongly overlapped bands in the CH stretching region, four Q-branches at 3021, 3007, 2997, and 2989 cm^{-1}, and a broader feature between 2960 and 2900 cm^{-1} are clearly observed. These also imply the presence of two conformers in the vapor. Overall, the band positions and relative intensities compare favorably with the calculated positions and intensities. The spectrum confirms the presence of two conformers, but a conformer ratio could not be derived from the spectrum because of the extensive band overlap.

Isomerization of CH_3CH_2OCN. The uni- and bimolecular isomerization of CH_3CH_2OCN (**1**) was investigated in a "vacuum" and in solvents using the B3LYP/6-311+G(2d,2p) method and the PCM model. Results are summarized in Table 5 and Figures 3 and 4. Calculations predict that the barrier of the unimolecular isomerization in various solvents is between $\Delta G^{\ddagger} = 218.9$ (in a vacuum) and 195.7 kJ/mol (in DMSO), which seems to be too high to explain instability at room or lower temperatures. Search for potential bimolecular reactions revealed two reaction routes in all solvents, leading to the isomer (**2**) or to a dimeric product (DP), and also a third one in polar solvents, producing cyanate ion. Kinetic energy barriers of these reactions are 40−50 kJ/mol lower than those of the unimolecular processes (Table 5). Figure 4 shows that the formation of the isomer **2**, via TS2a, is thermodynamically more favored than the formation of DP, via TS2b, and the two OCN groups are practically exchanged between two molecules of **1** in this reaction. DP may be an intermediate for the formation of the

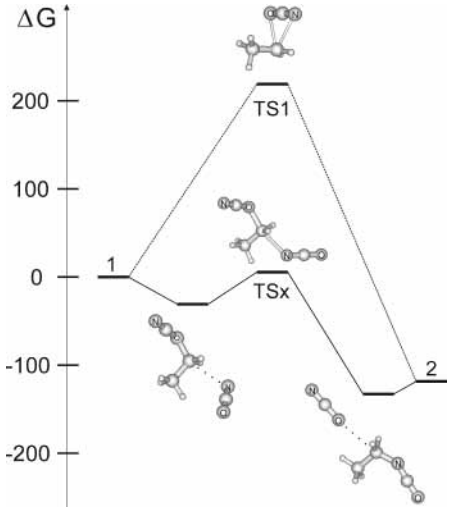

Figure 3. Unimolecular (top) and OCN^- ion catalized (bottom) isomerization of CH_3CH_2OCN (in a vacuum). Gibbs free energies are relative to that of CH_3CH_2OCN (**1**) and $CH_3CH_2OCN + OCN^-$ ion, respectively. Calculated at the B3LYP/6-311+G(2d,2p) level (ΔG in kJ/mol).

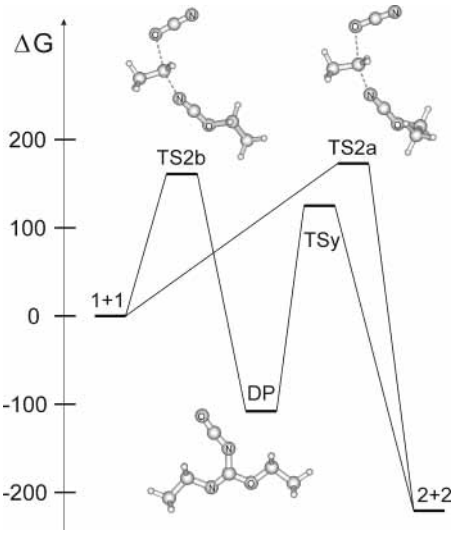

Figure 4. Bimolecular reaction of CH_3CH_2OCN in heptane. Gibbs free energies are relative to that of two molecules of CH_3CH_2OCN (1+1). Calculated at the B3LYP/6-311+G(2d,2p) level using PCM (ΔG in kJ/mol).

trimer, triethylisocyanurate, but the investigation of this is beyond the scope of this work. It is important to note the third reaction route in polar solvents, which produces OCN^- ion, via TS2c. Calculations show that OCN^- ion can effectively isomerize CH_3CH_2OCN, because the kinetic energy barrier for this process is small; it is $\Delta G^{\ddagger} = 93.0$ kJ/mol ($\Delta E^{\ddagger} = 62.5$ kJ/mol) in DMSO and decreasing by decreasing the polarity of the solvent (see Figure 3). The OCN^- ion is thus expected to be an isomerization catalyst for cyanat−isocyanat rearrangement; therefore, the isomerization of **1** is expected to be faster in polar than in apolar solvents. We note that the OCN^- ion is known to catalyze the trimerization of the isomerization product, **2**.[1,33]

Conclusion

The unstable ethyl cyanate molecule has been generated by passing *O*-ethyl thiocarbamate over yellow mercuric oxide. A pure sample was obtained by trapping and reevaporizing reaction products at 0 °C. Ethyl cyanate was characterized in the gas phase by infrared spectroscopy, and the IR spectrum indicates the presence of two conformers, the gauche and the trans form. Ab initio and DFT calculations provide the equilibrium structures and the ratio of these two conformers, and together with normal coordinate calculations, support the assignment of the spectrum. The isomerization of ethyl cyanate was studied in a vacuum and in various solvents using DFT and PCM. Calculations show that ethyl cyanate is unstable in the condensed phase because of bimolecular reactions. The isomerization is predicted to be faster and more complicated in a polar solvent than in an apolar medium because of the formation and catalytic action of cyanate ions.

Acknowledgment. We thank the Hungarian Scientific Research Fund and the Hungarian Academy of Sciences (OTKA Grant F022031, AKP Grant 98-69 2,4) for research grants in support of this work.

References and Notes

(1) Martin, D.; Niclas, H.-J.; Habisch, D. *Liebigs Ann. Chem.* **1969**, *727*, 10.
(2) *The Chemistry of Cyanates and their Thio Derivatives*; Patai, S., Ed.; Wiley: New York, 1977.
(3) Al-Juaid, S. S.; Al-Nasr, A. A. K.; Ayoko, G. A.; Eaborn, C.; Hitchcock, P. *J. Organomet. Chem.* **1995**, *488*, 155.
(4) Eaborn, C.; Lickiss, P. D.; Markuina-Chidsey, G.; Thorli, E. Y. *J. Chem. Soc., Chem. Commun.* **1982**, 1326.
(5) Martin, D. *Tetrahedron Lett.* **1964**, *39*, 2829.
(6) Martin, D.; Weise, A. *Chem. Ber.* **1966**, *99*, 976. Holm, A.; Huge-Jensen, E. *Acta Chem. Scand. B* **1974**, *28*, 705. Fischer, H.; Zeuner, S.; Ackermann, K.; Schubert, U. *J. Organomet. Chem.* **1984**, *263*, 201.
(7) Reich, P.; Martin, D. *Chem. Ber.* **1965**, *98*, 2063.
(8) Groving, N.; Holm, A. *Acta Chem. Scand.* **1965**, *19*, 443.
(9) Jensen, K. A.; Holm, A.; Wentrup, C. *Acta Chem. Scand.* **1966**, *20*, 2107.
(10) Sakaizumi, T.; Mure, H.; Ohashi, O.; Yamaguchi, I. *J. Mol. Spectrosc.* **1989**, *138*, 375.
(11) Urban, J.; Nowek, A.; Venkatraman, R.; Babinec, P.; Leszczynski, J. *Struct. Chem.* **1998**, *9*, 161.
(12) Pasinszki, T.; Westwood, N. P. C. *J. Phys. Chem.* **1995**, *99*, 1649.
(13) Davies, W.; Maclaren, J. A. *J. Chem. Soc.* **1951**, 1434.
(14) Frisch, M. J.; Trucks, G. W.; Schlegel, H. B.; Scuseria, G. E.; Robb, M. A.; Cheeseman, J. R.; Zakrzewski, V. G.; Montgomery, J. A., Jr.; Stratmann, R. E.; Burant, J. C.; Dapprich, S.; Millam, J. M.; Daniels, A. D.; Kudin, K. N.; Strain, M. C.; Farkas, O.; Tomasi, J.; Barone, V.; Cossi, M.; Cammi, R.; Mennucci, B.; Pomelli, C.; Adamo, C.; Clifford, S.; Ochterski, J.; Petersson, G. A.; Ayala, P. Y.; Cui, Q.; Morokuma, K.; Malick, D. K.; Rabuck, A. D.; Raghavachari, K.; Foresman, J. B.; Cioslowski, J.; Ortiz, J. V.; Stefanov, B. B.; Liu, G.; Liashenko, A.; Piskorz, P.; Komaromi, I.; Gomperts, R.; Martin, R. L.; Fox, D. J.; Keith, T.; Al-Laham, M. A.; Peng, C. Y.; Nanayakkara, A.; Gonzalez, C.; Challacombe, M.; Gill, P. M. W.; Johnson, B. G.; Chen, W.; Wong, M. W.; Andres, J. L.; Head-Gordon, M.; Replogle, E. S.; Pople, J. A. *Gaussian 98*, revision A.7; Gaussian, Inc.: Pittsburgh, PA, 1998.
(15) Pulay, P.; Fogarasi, G.; Pongor, G.; Boggs, J. E.; Vargha, A. *J. Am. Chem. Soc.* **1983**, *105*, 7037.
(16) Fogarasi, G.; Zhou, X.; Taylor, P. W.; Pulay, P. *J. Am. Chem. Soc.* **1992**, *114*, 8191.
(17) Coffin, J. M.; Pulay, P. *Program TRA3*; Department of Chemistry and Biochemistry, University of Arkansas: Fayetteville, AR, 1989.
(18) Pulay, P. In *Applications of Electronic Structure Theory, Modern Theoretical Chemistry*; Schaefer, H. F., III., Ed.; Plenum: New York, 1977; Vol. 4, p 153.
(19) Pongor, G.; Fogarasi, G.; Magdó, I.; Boggs, J. E.; Keresztury, G.; Ignatyev, I. S. *Spectrochim. Acta* **1992**, *48A*, 111.
(20) Pongor, G. *Program SCALE3*; Department of Theoretical Chemistry, Eötvös Loránd University: Budapest, Hungary, 1993.
(21) Pulay, P.; Török, F. *Acta Chim. Hung.* **1965**, *44*, 287.
(22) Keresztury, G.; Jalsovszky, G. *J. Mol. Struct.* **1971**, *10*, 304.
(23) (a) Sakaizumi, T.; Sekishita, K.; Furuya, K.; Tetsuda, Y.; Kaneko, K.; Ohashi, O.; Yamaguchi, I. *J. Mol. Spectrosc.* **1993**, *161*, 114. (b) Sakaizumi, T.; Mure, H.; Ohashi, O.; Yamaguchi, I. *J. Mol. Spectrosc.* **1990**, *140*, 62.
(24) Zylka, P.; Mack, H.-G.; Schmuck, A.; Seppelt, K.; Oberhammer, H. *Inorg. Chem.* **1991**, *30*, 59.
(25) Seppelt, K.; Oberhammer, H. *Inorg. Chem.* **1985**, *24*, 1227. Oberhammer, H.; Seppelt, K.; Mews, R. *J. Mol. Struct.* **1983**, *101*, 325.
(26) Koput, J.; Winnewisser, B. P.; Winnewisser, M. *Chem. Phys. Lett.* **1996**, *255*, 357.

(27) Pasinszki, T.; Westwood, N. P. C. *J. Phys. Chem.* **1995**, *99*, 6401.
(28) Pasinszki, T.; Westwood, N. P. C. *J. Phys. Chem. A* **1998**, *102*, 4939.
(29) Pasinszki, T.; Westwood, N. P. C. *J. Phys. Chem.* **1996**, *100*, 16856.
(30) Rauhut, G.; Pulay, P. *J. Phys. Chem.* **1995**, *99*, 3093.
(31) Baker, J.; Jarzecki, A. A.; Pulay, P. *J. Phys. Chem. A* **1998**, *102*, 1412.
(32) The theoretical PR separations for pure *A*-, *B*-, and *C*-type bands using the computed rotational constants and the equations of Seth-Paul (Seth-Paul, W. A. *J. Mol. Struct.* **1969**, *3*, 403) are *A*: 15.8 and 14.0; *B*: 13.1 and 11.7; *C*: 23.7 and 21.0 cm^{-1} for the gauche and trans forms, respectively.
(33) Arnold, R. G.; Nelson, J. A.; Verbane, J. J. *Chem. Rev.* **1957**, *57*, 47.